

Space-Borne-Synthetic Aperture Radar (SAR) System For Real Time Surveillances Of Earth Surface For Detection And Management Of Flood Disaster In Indian Sub-Continent

Arun Kumar Verma^{1*}, Ranbir Nandan², Aditi Verma³

¹Ex-Senior Scientist (DRDO) and Director, Vidyadaan Institute of Technology & Management, Aryabhata Knowledge University, Dumraon, Bihar, India

²Associate Professor and MLC (Bihar Legislative Council), Geology Department, B.N. College, Patna University, Patna, Bihar, India

³Engineer, Qualcomm India, Hyderabad, India

How to cite this paper: Verma, A.K. et al. (2018) Space-Borne-Synthetic Aperture Radar (Sar) System For Real Time Surveillances Of Earth Surface For Detection And Management Of Flood Disaster In Indian Sub-Continent. *Journal of Applied Mathematics and Computation*, 2(5), 166-177.
<http://dx.doi.org/10.26855/jamc.2018.05.001>

*Corresponding author: Arun Kumar Verma, Vidyadaan Institute of Technology & Management, Aryabhata Knowledge University, Dumraon, Bihar, India
E-mail:arun@vidyadaan.org

Abstract

Earth Observation System consisting of remote sensing satellite in optical and microwave spectrum provides the information of different environmental and earth surface parameters by mapping and monitoring the earth surface for natural disasters such as earth quake, landslides, floods and forest fire apart from natural resource management. The remote sensing satellite images of multi-spectral sensors in the optical spectrum are affected by weather conditions due to clouds and rains as well as climatic conditions, restricting its application during clear sky conditions apart from limiting its image acquisition during the day time only. The development in the space borne synthetic aperture radar (SAR) technology and imaging techniques to reduce the repeat pass period using multi-SAR systems in orbits makes its suitable for real time monitoring and mapping of earth surface for the flood and water resource management due inherent cloud and rain penetrating capability as well as backscattering properties of radar signals in different frequency band. The recent development of space-borne SAR systems in bi-static and multi-static configuration by different space agencies ensures the availability of multi-sensor SAR in different microwave radar bands for the development of space-based flood disaster management system. The inherent characteristics to generate high contrast in SAR image between surfaces such as soil and water is due to very low backscattering coefficient of radar signals from water bodies acting as a mirror reflecting surface and earth surface gives higher backscattering coefficient due to surface roughness consisting of soil characteristics and vegetation, which increases the radar reflectivity of the surface. Major rivers in India like Indus, Ganga and Brahmaputra are snow-fed as well as monsoon rainfall dependent, while the other river basins are purely rainfall dependent. A large variability in the characteristics of rainfall has been observed over the basin in different seasons and months. The southwest (SW) monsoon, which brings about 80% of the total precipitation over the country, is critical for the availability of freshwater for drinking and irrigation. Flooding in rivers are caused due to excessive rainfall and discharge of water in the river basins leading to the overflow of the water submerging the landmass depending upon its terrain profile, river bed characteristics, raindrop size distribution and rainfall characteristics. In this paper, the concept of the bi-static and multi-static space-borne SAR sensors has been described for development of real time space-borne surveillance system for Indian Sub-continent as Disaster Management Sys-

tem (DMS), which can be used for flood detection and flood disaster management. The concept of geostationary radar illuminator and constellation of multi-SAR-satellites in LEO has been described.

Keywords

Remote Sensing Satellite, Bi-static and Multi-static SAR System, Radar Backscattering Coefficient, Flood Detection Techniques, Geostationary Radar Illuminator, Low Earth Orbit (LEO), Micro-SAR Receiver

1. Introduction

Earth Observation System consisting of sensors in multi-spectral (optical) and microwave range provides an important source of information for mapping and monitoring of changes on the earth surface such as forest fires, floods, earthquake, and landslides as surveillance to the earth surface for the management of different phases of disaster and early warning system apart from national natural resource management. The applications of satellite images of multi-spectral sensors in optical spectrum is not suitable for detection and monitoring of flood during rainy season and clouds in the sky due to non-penetrating capability of signals restricting its applications during clear sky condition. The other limitation of multi-spectral sensors in optical spectrum is its acquisition of satellite imageries during day time only.

The development of space-borne Synthetic Aperture Radar (SAR) technology due to its imaging capability during day and night as well as during the rainy period makes it most appropriate for monitoring and prediction of flood management in the recent years. One of the major advantages of SAR images is its characteristic to generate high contrast between surfaces such as soil and water due to very low backscattering coefficient of radar signals from water bodies acting as a mirror reflecting surface. Further, earth surface gives higher backscattering coefficient due to surface roughness, which consists of soil characteristics and vegetation, resulting into increased radar reflectivity of the surface. As a result, the flood areas appear darker in SAR images (Sandholt I. et al, 2000). Therefore, the comparison of multi-SAR images before and during the flooding provides the mapping of flooded areas with high degree of precision. The change detection techniques on multi-temporal SAR images provide information related the status of water surface of river system, an overflow stream and the flooding of the surrounding area (Vilches P. J., March 2013). The recent development of space borne SAR system is focused on reduction of the repeat pass period (revisit time) from 35 days to sub-days for acquisition of SAR images using bi-static or multi-static micro SAR receivers (payloads) on satellite in Low Earth Orbit (LEO) in fully active or semi-active configuration suitable for real time surveillances of the earth surface including the flood disaster management (Krieger G., Moreira A., June 2006).

Floods are one of the most common disasters in the world accounting for 40% of all natural disasters worldwide causing damage to agricultural crops, roads, and the loss of human lives. Many of the world's urban centers are in low-lying areas subject to flooding. Therefore, rapid identification and response to flooded areas is essential to avoid turning an environmental phenomenon into a potentially grave disaster. The spatial and temporal characteristics of rain rate and rain drop size distribution plays very important role to cause flooding in the river basin, apart from siltation from plain/ hilly areas of terrain. The rivers in India may be broadly classified into Himalayan, peninsular, coastal and inland drainage-basin rivers. The Himalaya is the main source of water for the rivers in the Indo-Gangatic plains. Ganga, Brahmaputra and Indus originate from the Himalayan snow and ice fields. Glaciers in the Himalayas cover an area of around 38,039 sq.km. The water yield from a higher Himalayan basin is roughly twice as high as that from an equivalent basin located in the peninsular part of India. The Himalayan region and its foothills covering the adjoining plain area of Ganga River basin experiences thunderstorm and convective rain fall of very high rain rate intensity frequently, which is responsible to cause flooding in the Ganga river basin and its catchment area, apart from melting of Glacier (Singh A.K., Hasnain S.I., 1998; Goswami D.C., 1985). The southwest (SW) monsoon, which brings about 80% of the total precipitation over the country, is critical for the availability of freshwater for drinking and irrigation (Benn D.I., Owen L.A., 1998). Flooding in rivers are caused due to excessive rainfall and discharge of water in the river basins leading to the overflow depending upon its terrain profile, river bed characteristics, raindrop size distribution and rainfall characteristics (Verma A.K, Nandan R., Singh S.K., Verma A., 28 May 2017).

In this paper, the characteristics of Indian river basins and rainfall characteristics including rain drop size distribution has been described for the understanding the causes of river floods. This paper explains the building blocks of SAR systems as well as river and rain characteristics for detection and monitoring of floods using space- based SAR sensors. In this paper, the concept of the bi-static and multi-static space-borne SAR sensors has been described for the development of space-borne SAR surveillance system for Indian Sub-continent as Disaster Management System (DMS). The concept of geostationary radar illuminator and constellation of multi-static SAR receiver on micro or nano-satellites in LEO or MEO has been described for real time space-borne SAR system for flood detection, monitoring and surveillances for disaster management.

2. Indian River Basins and Rainfall Characteristics

In India, river basins having catchment areas exceeding 20,000 sq. km are classified as major basins. The Ganga–Brahmaputra–Meghna (Barak) system is the largest amongst the major rivers. Three major basins such as Indus, Ganga and Brahmaputra are snow-fed as well as rainfall dependent, while the other river basins are purely rainfall dependent. Seven other medium-sized basins of Sabarmati, Mahi, Narmada and Tapi rivers flowing west and the Subarnarekha, Brahmani, Baitarani and Cauvery rivers flowing east together cover only 15% of the total drainage area of India. The water yield from a high Himalayan basin is roughly twice as high as that from an equivalent basin located in the peninsular part of India. The Himalayan sector receives 500 cm of rainfall per year, the lower ranges receiving more than the higher area. Monsoonal rains from June to September account for 60-70% of the annual rainfall. Ganga and Brahmaputra have comparable discharges, but the Ganga meanders while the Brahmaputra is a braided river. Since the Himalayan rivers traverse through poorly consolidated sedimentary rocks affected by folds, faults and thrusts, there is greater erosion and removal of silt in these rivers (Goswami D.C.1985). The Himalaya plays a very significant role in influencing the climate of India. The Himalayan climate is largely controlled by the mid-latitude westerlies and Indian Summer Monsoon (ISM). The Eastern Himalaya is predominantly influenced by the ISM (Benn D.I., Owen L.A., 1998). The western Himalaya is dominated by the mid-latitude westerlies and receives snowfall during winter. Annual rainfall in India generally reflects the features of the monsoon rainfall fluctuation. Winter (January–February) rainfall is of some significance in extreme northern India and the southeast peninsula and summer (March–May) rainfall is of significance in northeastern India and the extreme southwest peninsula. However, post-monsoon (October–December) rainfall is of considerable significance in the southern peninsula. A large variability in the characteristics of rainfall has been observed over the same basin in different seasons and months. The southwest (SW) monsoon, which brings about 80% of the total precipitation over the country, is critical for the availability of freshwater for drinking and irrigation. Rainfall time series analysis based on river basin average rainfall (1813 to 2001) provides temporal features of rainfall characteristics. There are increasing trend of rainfall over Indus, Ganga, Brahmaputra, Krishna and Cauvery river basin from 1954, 1993, 1988, 1953 and 1929 onward respectively. Similarly, there are decreasing trend of rainfall over Sabarmati, Mahi, Narmada, Tapi, Godavari and Mahanadi river basin from 1960, 1964, 1950, 1965, 1964 and 1962 onwards respectively. The trend analysis of rainfall, temperature and other climatic variables on different spatial scales will help in the construction of future climate scenarios (Singh A.K., Hasnain S.I., 1998)

3. Rain Drop Size Distribution (RDSD) Spectra for Indian Climate

Rainfall characteristics depend on rain rate, rain drop size distributions, spatial and temporal characteristics of rain rate. Research Scientist such as Laws and Parsons (LP) and Marshal and Palmer (MP) derived the rain drop size distribution (RDSD) based on the measurement of rain drop size data for temperate climate, which follows the exponential distribution. For tropical climate like Indian sub-continent, the characteristics of rain drop size distribution were measured by many research scientists, which follow lognormal rain drop size distribution. Verma et al developed log-normal rain drop size distribution (RDSD) model for Indian climate based on the measurement of 4200 and 1100 rain events (1 minute duration) of rain drop size data using Distrometer during 1989-93 at Defence Electronics Applications Lab (DEAL), Dehradun. The Distrometer is basically an impact sensor, which classifies the rain drop size (0.25 mm to 5 mm diameter) based on its impact signal into 20 different drop sizes and collects the rain drop of different sizes for 1-minute duration as single rain event. Indian Space Research Organisation (ISRO) also conducted the measurement of rain drop size for various location of Indian region such as Shillong, Kharagpur, Ahmedabad, Trivendrum, and Hassan during 2004-2007 and developed log-normal RDSD model. Further, the measurement of RDSD was conducted during 2003 to 2005 between Stations in Eastern and Western coasts of India with special reference to Thiruvananthapuram, Kochi (western stations) and Sriharikota (Eastern station). Rain drop size distribution (RDSD) was also measured at Raichur (Raichur-Belgaum: Karnataka, India), a Southern Indian tropical region from 2009 – 2012, which follows log-normal

RDS. It is observed based on the analysis of measured data that the rainfall duration at low intensity is maximum and decreases exponentially with increasing intensity. Therefore, higher rain rate events are very less compared to the lower rain rate events. The rain drop size distribution confirms log-normal distribution as number of rain drops increases rapidly and then decreases gradually (Jassal B.S., Verma A.K., Singh L., 1994; Verma A.K., Jha K.K., 1996; Vidyarthi A., Jassal B.S., Gowri R., Shukla A.K., 2012). The number of rain drops increases with the increase of rainfall, but with the intense rainfall at Shriharikota and Kochi confirms the increase of rain drops in contrary to increase of rain drop sizes as well as rain drops at Thriuvanthapuram. Law and Parsons RDS Model suits to temperate region, whereas log-normal or gamma distribution fits to the tropical region based on measurement conducted by researcher in India, Brazil, Nigeria, Singapore and Malaysia. The tropical rain drop size distribution follows log-normal distribution of rain drop sizes and can be written as

$$N(D_i) = \frac{N_T}{\sigma D_i \sqrt{2\pi}} \exp[-0.5\{(\ln D_i - \mu)/\sigma\}^2] \quad (1)$$

Where, N_T is the total number of drops of all sizes, μ and σ are the mean and standard deviation of D_i (drop size i -channel, i varies from 1 to 20 drop sizes). Here, N_T , μ and σ are the functions of rain rate and can be written as

$$N_T = a_0 R^{b_0}; \mu = A_\mu + B_\mu \ln R; \sigma^2 = A_\sigma + B_\sigma \ln R \quad (2)$$

Using Distrometer data, one minute rain rate for each rain event can be written as

$$R = 10\pi/A_i \sum d_i^3 n_i \quad (3)$$

Where, A_i is the area of sensor and n_i is the number of drops for the i_{th} channel. Hence for each corresponding rain rate, the number of drops per unit volume per diameter interval $N(D_i)$ can be written as

$$N(D_i)\Delta D_i = 10^4 [N_i/A_i T v_i] \quad (4)$$

The log-normal RDS model developed based on the rain drop size data measurement at different locations in the Indian tropical region have different value of coefficients of N_T , μ and σ and given in Table 1.

Table 1. Value of Coefficients for different locations

Location (Latitude, Longitude)	a_0	b_0	A_μ	B_μ	A_σ	B_σ
Dehradun (30.318°N, 78.029°E)	169.05	0.2937	-0.05556	0.13096	0.30042	-0.023604
Ahmedabad (23.03°N, 72.58°E)	149.3799	0.3467	-0.1380	0.1569	0.0625	0.0079
Tri vandrum (8.5°N, 76.9°E)	176.7605	0.3178	0.1934	0.1684	0.0692	0.005
Shillong (25.566°N, 91.883°E)	170.3792	0.26	0.1925	0.1831	0.0738	0.0059
Kharagpur (22.33°N, 87.323°E)	140.8542	0.2994	0.1417	0.1716	0.0744	0.0064
Hassan (13.012°N, 76.068°E)	225.9998	0.3041	0.2557	0.1615	0.0683	0.0097

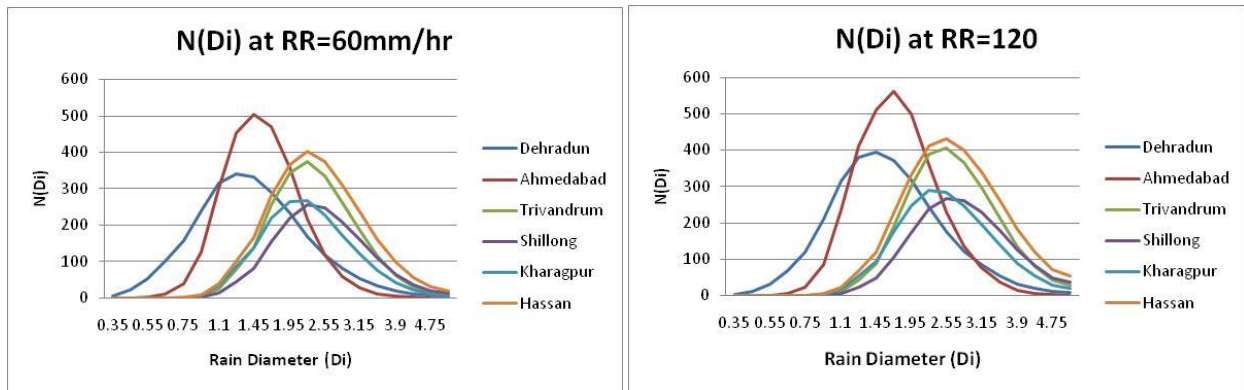


Figure 1. Variation of RSD Spectra in different locations at 60 mm/hr rain and 120 mm/hr rain rate

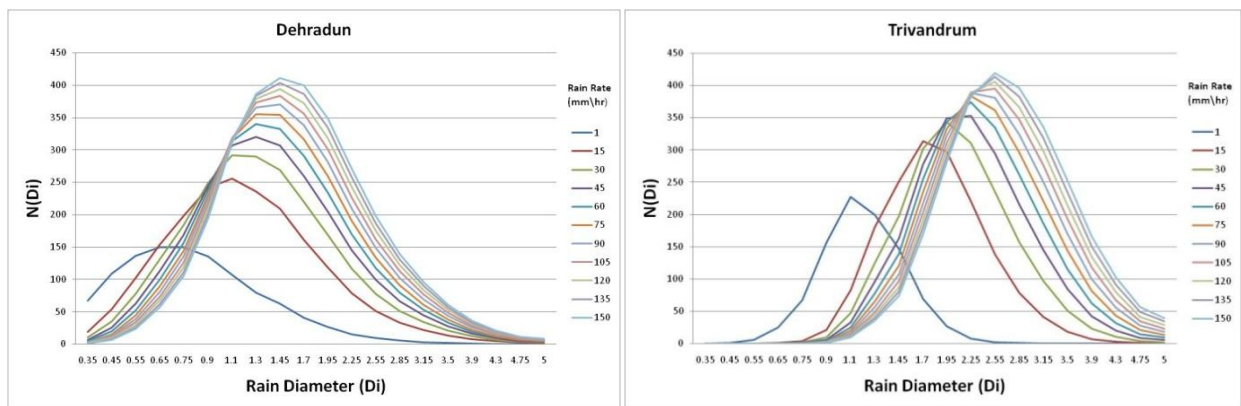


Figure 2. Variation of RSD Spectra with rain rate at Dehradun and Trivandrum

Figure 1 explains the variation of rain drop spectra at different locations at the same rain rate event. The analysis of different models based on the RSD measurement shows maximum $N(D)$ for Ahmedabad and rain characteristics consists of smaller rain drops between 0.55mm and 3.15 mm with the variation of rain rate compared to other locations. Rain drop size distribution pattern of Shillong and Kharagpur follows the similarity and consists of larger rain drops between 0.75 mm and 4.5 mm for the same rain events compared to Dehradun and Ahmedabad. Similarly, RSD spectra of Trivandrum and Hassan consist of larger rain drop sizes due to similar climatic condition. The rain drop size spectra for Dehradun consists of both smaller and larger rain drop sizes with moderate $N(D)$ values from 0.35mm to 4.5 mm drop size due to variation the formation of rain process in the Himalayan Climatic condition. Figure 2 explains the variation of rain drop spectra with rain rate at Dehradun and Trivandrum. The characteristics of $N(D)_{max}$ and corresponding rain drop size (D) varies with rate differently for both locations. The rain drop size (D) for $N(D)_{max}$ varies with rate from 0.65mm to 1.75 mm for Dehradun, however, the corresponding rain drop size (D) for $N(D)_{max}$ varies from drop size 1.1 mm to 2.85 mm for the same rain rate. The variation in the drop size spectra for different location is due to variation in the climatic condition and the process of rain formation causing the rain events.

4. Synthetic Aperture Radar (SAR)

Synthetic Aperture Radar (SAR) is basically side looking radar having an active microwave system composed of a transmitter and a receiver for imaging the large area of earth surface frequently at a reasonable resolution. The principle of SAR has been developed by the use of an advanced signal processing technique for creating a large synthetic aperture, which allows fine resolution of radar imaging and phase preservation during the single pass or repeat pass SAR imaging (Verma A.K., Goyal R.K., 1996). Space-borne or air-borne SAR imaging system are capable of imaging the earth surface with night and day and all weather operability in different radar bands in the microwave and mm wave frequencies. In space-borne SAR systems, the backscattered signal depends on (a) Transmitted frequency (b) polarization of trans-

mitted and received signals (c) incidence angle between transmitted signal and terrain surface (d) topographic slope (e) dielectric properties of earth surface and sub-surface materials. Radar signals interact with dielectric media such as earth surface, vegetation, soils, ice, waters depending upon their frequency, polarization, incidence angle, penetration capability and provides brightness/ tone in the radar (SAR) image depending upon backscattering properties with material target/ scene. These properties are used for identification/ classification/ mapping of earth surface due to subsidence/ earthquake/ floods/ landslides/ forest fire etc. In the SAR imageries, dominant factor is strength of amplitude of backscattered signals, which determines surface roughness of earth terrain and classifies earth surface as smooth, slightly rough, moderately rough or very rough depending on radar wavelength and angle of incidence of radar signal. It means that same earth surface, which appears smooth at longer wavelength may be rough at shorter wavelengths (Martin J., 2015 ; Verma A.K, Nandan R.,Singh S.K., Verma A., 28 May 2017). The strength of backscattered signals indicates the tone of the image such as rough targets appears bright and a smooth target appears dark e.g. Sea surface/ river surface at longer wavelength appears dark in radar image in comparison to earth surface. The intensity of radar backscattered is usually expressed in dB (decibel). The value of backscattered signal varies from +5dB for very rough surface to -40dB for very smooth surface (Sandholt I, Nyborg L., Fog B., Lo M., Boucum O.,Rasmussen K.,2000).

4.1 Characteristics of SAR Sensor

4.1.1 Roughness of the Surface: The Rayleigh criteria to establish the degree of surface roughness are used taking into account the wavelength value and the angle of incidence of the radar wave, and is expressed as follows. The object surface is considered smooth (not rough) if $h < \frac{\lambda}{8 \cdot \cos \theta}$, where h is the average height of the surface roughness (measured in cm), λ represents the wavelength of the incident radar energy (measured in cm), and θ represents the value of the angle of incidence of the wave on the object surface.

4.1.2 Effect of Radar Backscattering on SAR Images: The backscatter coefficient (σ^0) represents the effect of the earth's surface on the radar signal, means the percentage of the radar wave energy is reflected back to the radar from a 'cell or resolution unit' and is calculated as $\sigma^0 = \frac{\sigma}{Area}$. The value of σ^0 for a particular surface depends on various parameters of the earth surface such as geometry, roughness, the moisture content, and radar parameters such as wavelength, angle of incidence and polarization as given in Figure 3 and Table 2.

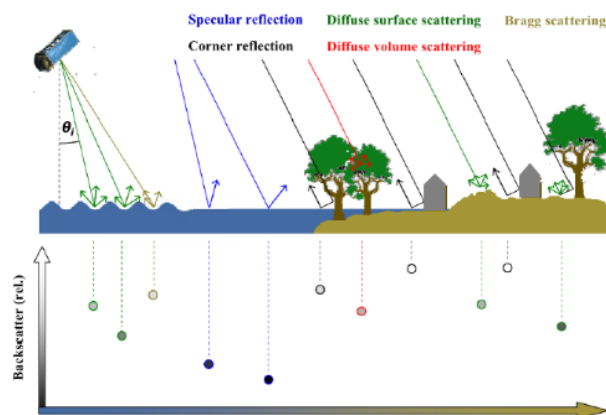


Figure 3. Radar Backscattering of radar signal

4.1.3 Potential Advantage of SAR Images for Flood Detection: Water bodies act as a mirror reflecting surface due to low backscatter coefficient and their low backscattered response looks like a dark area in SAR images. The earth, for its part, gives a much greater amount of radar energy due to the surface roughness and generates the high contrast between surfaces such as soil and water. For the particular case of water bodies, wind and waves or runoff can cause changes on the surface waves of water bodies and the wavelengths in the radar images are usually sensitive to surface wave in water

bodies causing enhanced backscattering and hence lowers the contrast between surfaces of water compared to the other cover. Due to this, SAR appears to be an ideal sensor for detecting flooding in extensive areas, since the backscattering signature is so distinctive for water compared to the vegetation. In the case of wetlands, the water affects the dielectric constant of the surface and therefore backscattering coefficient, which is of great importance in the application of SAR data. The behavior of the earth backscattering is regulated by the geometric features of the surface and the dielectric properties of the soil and its water content (humidity). The dielectric constant increases with soil moisture content influences the radar wavelength penetration. The longer the wavelength, the greater the sensitivity of the dielectric constant moisture content in soil. This means that in the L) band SAR images tend to be more sensitive to moisture in the soil than the bands of shorter wavelength such as C band or X-band.

Table 2. Backscattering coefficients of various target

Backscattering Coefficients (dBm/sqm)	Target
50	Point Target
20	Vehicles, Ships (Metallic)
01	Urban Area
-7	Forest
-10	Vegetation
-15	Short Grasses
-15 to -25	Water bodies
-22	Noise Image Limit
-30 to 50	Concrete, Bitumen

4.2 Modeling of SAR Back-Scattering for Detection of Flood/Water Bodies

SAR polarization is a key factor in flood detection and HH-polarized images are considered more adequate for flood detection than VV- or cross-polarized images due to the fact that HH-polarization gives the highest distinction in backscatter values between dry and wet forested areas. However, combining different polarizations can lead to improved flood maps, as HV polarization is less sensitive to surface conditions of water bodies.

4.2.1 Open Flooded Water : Open water behave as a perfect smooth surface for flood mapping for SAR system as reflects most radiance away from side-looking SAR sensors and generates virtually zero backscatter, thus making open water appear as dark on a SAR image. So, it becomes very convenient to detect water body due to the contrast with the surrounding rougher areas which generate more backscatter and appear brighter on SAR images. Short wavelengths show a higher contrast ratio between land and water than longer wavelengths, as the electromagnetic radiation only interacts with objects same or larger than its wavelength. Therefore, the longer the wavelength, the smaller the number of possible rough features on land that cause backscatter. Therefore, smooth land surfaces appear dark and similar to water on longer wavelength images. Consequently, shorter wavelength SAR images appear to be more suitable for open water detection purposes than those of longer wavelength. C-band SAR systems are widely used for environmental monitoring, and are proven to distinguish dry land from open water.

4.2.2: Flooded Vegetation: Each vegetation layer affects the radar signature due to different types of radar backscatter in wetland ecosystems. A forested area can be divided into three layers such as (a) a canopy layer which consists of small branches and foliage, (b) a trunk layer consisting of large trunks and branches, and (c) a ground layer, earth surface covered by water (Martin J., 2015). Floods under forest canopy can be detected by a strong rise in backscatter values in contrary to the backscattering from the same forested areas in dry conditions due to the reflection of the radar pulse from the horizontal water surface and backscattering from the trunks and branches of the vegetation, which results in strong signal return as shown in Figure 4(a). The backscatter mechanism from a flooded forested area, can be modeled as with an equation: $\sigma^o = \sigma_c^o + \alpha_c^2 (\sigma_m^o + \sigma_t^o + \sigma_s^o + \sigma_d^o)$. The total microwave backscatter (σ^o) consists of backscattered radiation from the canopy (σ_c^o), tree trunks (σ_t^o), surface (σ_s^o), double bounce from the trunks and surface (σ_d^o), and other multipath backscattering (σ_m^o). The highest influence on the total backscatter from flooded forest areas is given by the water-trunk reflection (σ_d^o) and the difference between backscatter coefficients obtained from flooded and non-flooded

conditions under forest canopy can be up to 10 dB. The canopy and trunk attenuation coefficient (α_c^2) is a function of radar frequency and derived from the transmissivity of the crown and trunk layers of the forest. X-band SAR refers to higher interference with foliage and canopy than lower frequencies in P- or L-band SAR, resulting into loss of canopy penetration ability for higher frequency SAR sensors. Therefore, lower frequencies such as L-band are generally preferred for forest flood mapping. As SAR image resolution is directly proportional to bandwidth, higher resolution imaging is possible in shorter wavelength bands like in X- or C-band compared to L-band. Thus, C-band SAR can provide a compromise between spatial resolution and canopy penetration for flood mapping.

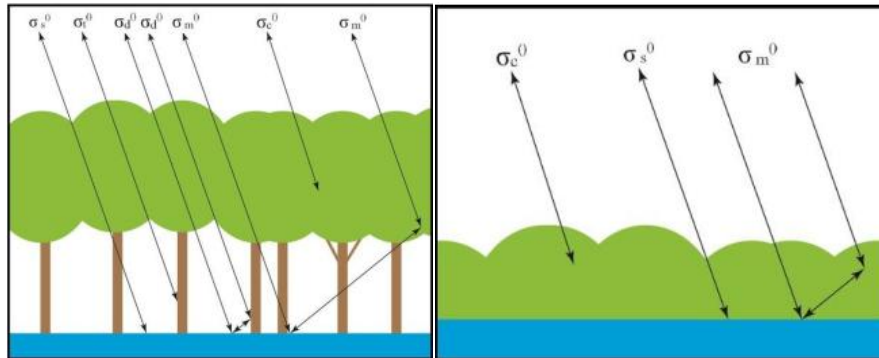


Figure 4(a). Flooded Vegetation, 4(b). Non-woody flooded Shrub

4.2.3 Non-Woody Flooded Shrub: These areas can be modeled similarly to flooded forested areas as shown in Figure 4(b) by eliminating all items on the trunk layer by simplified equation as $\sigma^o = \sigma_c^o + t_c^2 (\sigma_m^o + \sigma_s^o)$. The transmission coefficient (t_c^2) refers to the transmissivity of the vegetation canopy layer

4.3 Threshold Techniques for Change Detection for Flood Management

There are various image processing techniques to delimit area with water from SAR images. Traditionally, threshold is selected in SAR intensity images for getting the land and water separation in order to detect water bodies which differs with incidence angle. Rayleigh Criterion is considered for the measurement of water surface roughness due to low backscattering from water surface. Due to the horizontal nature of water surface, HH polarized SAR image provides better response compared with VV polarized SAR images. It is found that C and L band HH polarized SAR sensors are appropriate to detect flooded area with low plant canopy. However, X-band or C-band SAR sensors are better to detect water bodies under the vegetation, but P-band or L-band SAR signals penetrates in the canopy and interacts with trunk under forest environment for detection of flooded area. In order to detect flood from SAR images, five steps are required to follow such as (a) query of “crisis” and “reference” image (b) water backscattered statistical distribution (c) radiometric threshold of SAR image (d) region growing and (e) change detection for flood detection as given in Figure 5 (Vilches P. J., March 2013).

5.0 Bi-Static and Multi-Static SAR Sensors for Real Time Flood Management

Bi-static radar is defined as radar, where transmitter and receiver are spatially separated with considerable distance compared to the target-receiver or target-transmitter distance as large baseline. Bi-static radar was developed prior to the development of mono-static radar during 1930. Recently, bi-static radar has received interest in the development of space-borne bi-static and multi-static SAR due its potential to reduce the revisit (repeat orbit) time for monitoring the changes on the earth surface and different radar missions depending upon the repeat orbit and SAR payloads on satellite. Space-borne SAR payloads can be placed in the orbit into fully active or semi-active configuration based on both transmits and receives capability of signals. First European SAR satellite (ERS-1) was launched by European Space Agency at C-Band (VV) during 1991 for taking SAR images of Earth Surface having spatial resolution of 25m and repeat orbit cycle of 35 days as revisit time for taking SAR images. Similarly, ERS-1 (C-Band), JERS-1 (L-band), Radarsat-1 (C-band), ALOS-PALSAR (L-band) launched during 1995, 1992, 1995, 2002 respectively with a spatial resolution of 25m, 18m, 8m and 10m, and repeat orbit cycle of 35, 44, 24 and 46 days respectively, which are known as first generation space-borne-SAR sensors for earth observation system. Due to the revisit time of few weeks, these first generation

SAR systems found its limited applications for monitoring the changes on earth surface and risk and disaster management.

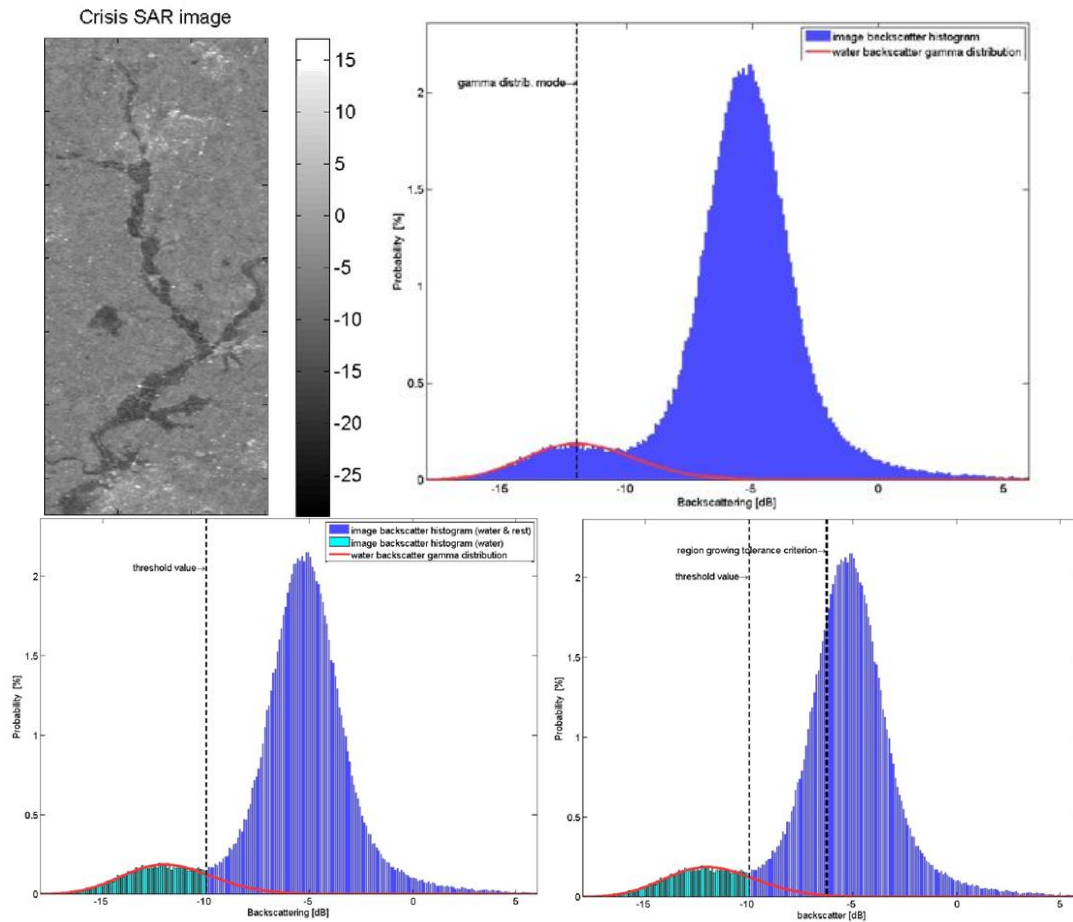


Figure 5. Threshold Techniques for flood detection

In fully active configuration, bi-static -SAR sensors have both transmitter and receiver as payloads on satellite in the LEO or MEO, which reduces the revisit time to several days and increase resolution of the images. German Space Agency developed and placed Terra-SAR-X in the sky as first bi-static radar from 2007 with repeat orbit cycle of 11 days and 1 m resolution, and known as 2nd generation SAR sensors as shown in Figure 6. First multi-static space-borne SAR sensors COSMO-SkyMed-1/4 with the constellation of four satellites is operational to provide resolution of 1m with 4 days repeat orbit. ISRO also launched first space-borne SAR sensor at C-Band in 2012. The distributed functionality of bi or multi-static SAR sensors provides natural large baseline, which supports small and low cost satellite (Krieger G., Moreira A., June 2006).

In the semi-active configuration of bi-static or multi-static SAR system, there will be one active SAR with transmitter and receiver as an active illuminator with one or more passive SAR receiver. This configuration requires deployable antenna of smaller sizes and reduced power demands of passive receiver. This potential lead to enable an accommodation of many SAR payloads on micro satellites in low earth orbits, which reduces the revisit time of SAR sensors to hours. In this semi-active configuration, SAR sensor from communication or navigational satellite illuminate the earth surface with very large radar footprint for backscattered signals, which are received by multi-SAR sensors (receivers) in placed in LEO for radar imaging as shown in Fig-7. In this case, satellite constellations allow for a modular design and shorten the development time for various missions. This results into highly reconfigurable and scalable satellite constellations for various remote sensing mission including the surveillance as well as risk and disaster management system in the sky.

The flexible imaging geometry of space-borne SAR sensors in multi-static configuration allows multi-missions to dynamically adapted to different operational tasks. The distributed satellite constellations have the potential to reduce the revisit time substantially based on the number of multi-SAR sensors in the LEO in conjunction with geo-stationary illuminator shown in Figure 7 and Figure 8. (Krieger G., Moreira A., June 2006; Verma A.K, Nandan R., Singh S.K., Verma A., 28 May 2017).



Figure 6. Space-borne SAR system in fully active configuration

This concepts (a) allows systematic reduction of the revisit time by increasing the number of low cost passive SAR receivers (b) upgradable to other imaging modes like cross-track interferometry or sparse aperture sensing (c) multi-missions by sharing the same SAR illuminator, which reduces the cost of each individual mission significantly and (d) in contrast to mono-static SAR, a ground resolution of 3 m (X-Band) can also be achieved in forward, downward and backward direction. The revisit time of multi-static-SAR satellite constellations can be optimized to frequent monitoring of selected ground area by (a) choosing appropriate orbit (MEO or LEO). It is possible to cover the given area up to five times within two days repeat cycle and (b) the revisit time below one hour can be achieved with a moderate number 10 SAR receivers as shown in Figure 8. Third generation Space-borne semi-active SAR sensors have the potential for the development of near real time disaster management system or traffic management system for the selected ground area (Krieger G., Moreira A., June 2006).

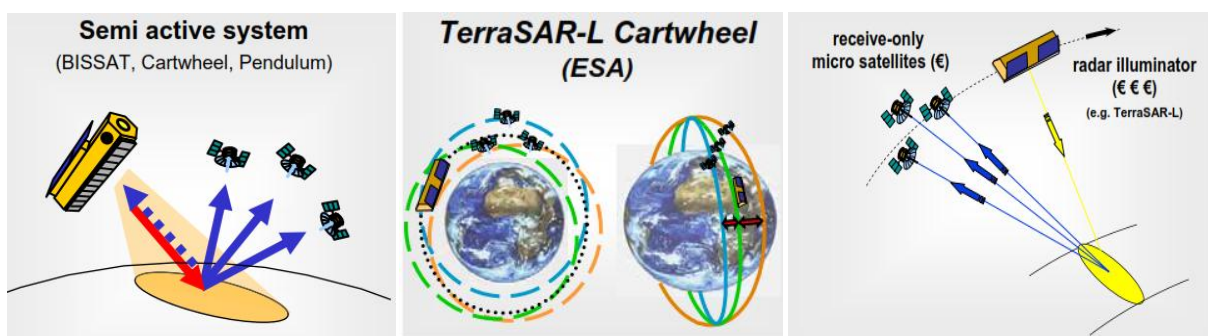


Figure 7. SAR system in semi-active configuration with TerraSAR and Geostationary Radar Illuminator

6. Conclusion

Several space-borne bi-static and multi-static SAR configurations are functional for different applications such as frequent monitoring of selected area of earth surface (flood and landslide), cross track interferometry, differential interferometry, wide swath high resolution imaging and scene classification/ traffic monitoring. A combination of geostationary radar illuminator with multiple SAR receivers in low earth orbits can perform multiple missions (task) in cost efficient way due to frequent monitoring capability for the revisit time of the same area below 1 hour duration, depending upon the appropriate design of constellation of specific number of micro / small SAR receiver satellites t involved for the particular mission. The constellation of 30 small SAR receiver satellites in the low earth orbit is capable to the reduce the revisit time below one hour for the European continent. The configuration of constellation of SAR receivers can be up-

graded or reconfigured for various remote sensing applications such as along-track or cross-track interferometry, high resolution wide swath imaging and space-borne tomography for real 3-D imaging of volume scatterers. Bi and multi-static SAR constellation in LEO have the potential to use the forward scattered signals, which increases the SNR by more than 10dB and increase the access region for new applications of data fusion. One of the important applications of multi-static SAR receivers in LEO is the single pass SAR interferometry for simultaneous data acquisition with multiple SAR receivers eliminating atmospheric disturbances and temporal de-correlation errors, which limits the performance of repeat pass SAR interferometry.

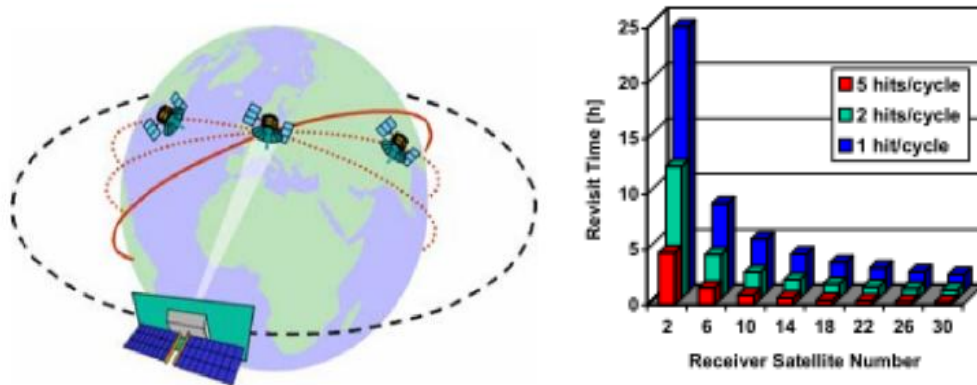


Figure 8. Frequent Monitoring with bi-static SAR satellite constellation. Left: Geostationary radar illuminator with LEO receivers. Right: Revisit times for local acquisition scenario (X-band SAR System, Transmit Power: 1KW, Transmitter antenna size: 100sqm , SAR receiver antenna size: 6sqm, SAR receiver altitude : 400Km (LEO), Ground range and azimuth resolution: 3m)

References

- [1] Benn D.I., Owen L.A., 1998. The role of the South Asian monsoon and the mid-latitude westerlies in controlling Himalayan glacial cycles: review and speculative discussion. *Journal of the Geological Society, London*, 155, pp 353-363.
- [2] Goswami D.C., 1985. Brahmaputra River, Assam, India: Physiographic, Basin denudation and Channel Aggradation. *Water Resource Research American Geophysics Union*, 21, pp 959-978.
- [3] Jassal B.S., Verma A.K., Singh L., 1994. Rain drop size distribution and attenuation for Indian climate. *Indian Journal of Radio and space Physics*. Vol 23, pp 193-196.
- [4] Krieger G., Moreira A., June 2006. Space-borne Bi- and Multi-static SAR: Potential and Challenges" *IEE Proc.-Radar Sonar Navigation.*, Vol. 153 (3), pp 184-198.
- [5] Martin J., 2015. Synthetic Aperture Radar based flood mapping in the Alam-Pedja Nature Reserve in years 2005-2011. Master thesis in Geo-informatics and Cartography, Institute of Ecology and Earth Science, University of Tartu
- [6] Singh A.K., Hasnain S.I., 1998. Major ion chemistry and weathering control in a high altitude basin: Alaknanda River, Garhwal Himalaya, India. *Journal of Hydrological Science*, 43(6), pp 226-228.
- [7] Sandholt I., Nyborg L., Fog B., Lo M., Boucum O., Rasmussen K., 2000. Remote sensing techniques for flood monitoring in the Senegal River valley. Submitted to *Danish Journal of Geography, Senegal Special issue*.
- [8] Verma A.K., Jha K.K., 1996. Rain drop distribution model for Indian Climate. *Indian Journal of Radio and Space Physics*, Vol 25(1), pp 15-21.
- [9] Verma A.K., Goyal R.K., 1996. Mathematical Formulation for estimation of Base-line in SAR Interferometry. *SADHNA: Academy Proceeding of Engineering Science*, Vol. 21, pp 511-522.
- [10] Vidyarthi A., Jassal B.S., Gowri R., Shukla A.K., 2012. Regional variability of RDS model in India. *Progress in Electromagnetics Research Letters*. Vol -34, P 123-135.
- [11] Vilches P.J., March 2013. Detection of area affected by Flooding River using SAR Images. Master in Space Applications for Emergency Early Warning and Response. CONOE, IG.
- [12] Verma A.K., Nandan R., 25-26 February 2017. Applications of SAR Imaging Technology for monitoring the characteristics flow of river Ganga and flood management. International Conference on "Incessant Ganga", Organized by

WALMI, Government of Bihar, Patna , PP-47-48.

[13] Verma A.K, Nandan R.,Singh S.K., Verma A., 28 May 2017. Space-borne Synthetic Aperture Radar (SAR) System for near real time detection and monitoring of flood in eastern region of India. International Seminar on Flood and Water Resource Management in the eastern region of the Indian Sub-continent, Organised by Indian Engineers Association, Patna, pp 40-52.